Control of MEMS Disc Resonance Gyroscope (DRG) using a FPGA Platform

Didier Keymeulen, Chris Peay, David Foor, Tran Trung[2], Alireza Bakhshi[3], Phil Withington, Karl Yee, Rich Terrile
[1]Jet Propulsion Laboratory, MS 303-300, 4800 Oak Grove Dr., Pasadena, CA 91109, USA; [2] University of California at Berkeley, [3] B&A Engineering Inc., 736 S. Walnut Ave, Sand Dimas, CA 91773
818-354-4280
didier.keymeulen@jpl.nasa.gov

Abstract—Inertial navigation systems based upon optical gyroscopes tend to be expensive, large, power consumptive, and are not long lived. Micro-Electromechanical Systems (MEMS) based gyros do not have these shortcomings; however, until recently, the performance of MEMS based gyros had been below navigation grade. Boeing and JPL have been co-operating since 1997 to develop high performance MEMS gyroscopes for miniature, low power space Inertial Reference Unit applications[12]. The efforts resulted in demonstration of a Post Resonator Gyroscope (PRG). This experience led to the more compact Disc Resonator Gyroscope (DRG) for further reduced size and power with potentially increased performance. Currently, the mass, volume and power of the DRG are dominated by the size of the electronics. This paper will detail the FPGA based digital electronics architecture and its implementation for the DRG which will allow reduction of size and power and will increase performance through a reduction in electronics noise. Using the digital control based on FPGA, we can program and modify in real-time the control loop to adapt to the specificity of each particular gyro and the change of the mechanical characteristic of the gyro during its life time.

TABLE OF CONTENTS

1. INTRODUCTION

Future NASA missions would benefit tremendously from an inexpensive, navigation grade, miniaturized inertial measurement unit (IMU), which surpasses the current state-of-the art in performance, compactness (both size and mass) and power efficiency. Towards this end, under current development at JPL's MEMS Technology Group are several different designs for environment tolerant [10], high performance, low mass and volume, low power MEMS gyroscopes. The accuracy with which the rate of rotation of micro-gyros can be determined depends crucially on the properties of the resonant structure. It is both difficult and expensive to attempt to achieve these desired characteristics in the fabrication process, especially in the case of small MEMS structures, and thus one has limited overall sensor performance due to un-avoidable fabrication inaccuracies.

The accuracy with which a given vibratory gyroscope can determine the true inertial rate is crucially dependent on the properties of the two degree-of-freedom resonator. The problem with tracking orientation using only gyros is drift such as gyro bias which creates a steadily growing angular error, gyro white noise and gyro bias instability [13]. Today's commercial grade gyros (devices used in automobiles, camcorders) can only be used for a minute before the drift becomes distracting and the user needs to reset the orientation tracker. Tactical-grade gyros used in short-range missile guidance are good enough for head-tracking for more than 20 minutes. Navigation-grade gyros are required for space applications. Unfortunately, the price, weight and power ratio between navigation, tactical and commercial-grade gyros follows the performance ratio. MEMS gyroscopes will be gradually closing in on the performance using techniques presented in the paper.

One way to reduce the rate drift is to increase the sensitivity or scale factor relating volts out to radians per second of inertial input [9]. The scale factor is maximized when the resonant frequencies of the two modes of freedom of the MEMS gyroscope are identical. Symmetry of construction is necessary to attain this degeneracy. However, despite a symmetric design, perfect degeneracy is never attained in

[1] 1-4244-1488-1/08/$25.00 ©2008 IEEE
[2] IEEEAC paper #1613, Version 2, Updated December 16, 2007

practice. Many methods have been developed for tuning MEMS post-resonator gyroscopes. For example [1] and [2] use adaptive and closed-loop methods, while [3] changes the frame of the pick-off signal. Our approach of gyro tuning is achieved through an electrostatic biasing approach [11]. This approach consists of applying bias voltages to built-in tuning pads to electrostatically soften the mechanical springs. Because of the time consuming nature of the tuning process when performed manually, in practice any set of bias voltages that produce degeneracy is viewed as acceptable at the present time. Thus a need exists for reducing the time necessary for performing the tuning operation, and for finding the optimally tuned configuration, which employs the minimal maximum tuning voltage.

This paper describes FPGA based digital electronics architecture for the DRG with augmented portability for future designs and implementations. The digital implementation allows through a graphical user interface to tune the gyroscope through bias voltage [11] and to program the digital filter and gains used in the drive loop and counterbalance loop.

This paper is organized such that Section 2 describes the mechanics of the MEMS micro-gyro, Section 3 describes the closed-loop hardware platform and the results of our preliminary experiments, and Section 4 describes future directions and summarizes the project results.

2. MECHANICS OF MEMS MICRO GYRO

JPL's Disc Resonator Gyroscope (DRG), shown in Figure 1, measures 11.4 x 11.4 x 1.3 mm, and is a high performance, compact and robust MEMS gyroscope. The in-run bias stability of this device has been measured at 0.25 deg/hr.

An exploded view of the DRG is illustrated in the figure above. Multiple narrow periodic slot segments etched through a planar wafer disc (blue) simultaneously define a unique in-plane resonator structure and a matching large area electrode array (green) for capacitive sense and actuation having very high area efficiency. A sinusoidal voltage applied to one set of electrodes drives the ring structure into a quadruple mode of oscillation (mode #1). This motion couples to the Coriolis force, exciting the second, degenerate, quadruple mode (mode #2) of the two dimensional ring structure. A feedback voltage signal applied to a second set of electrodes (rotated from the first by 45°) suppresses the motion of the second mode. A direct proportionality exists between the Coriolis rate input and the feedback voltage; thus, the rotation rate of the sensor can be extracted from a measurement of the feedback voltage.

The high degree of designed-in symmetry of the DRG ensures minimal coupling to external disturbances through the package. The centrally mounted resonator supports two degenerate elastic inertial waves for Coriolis sensing having zero momentum relative to the base plate so that all of the modal momentum remains locked within the resonating medium. This feature, which eliminates noisy and non-repeatable anchor losses, and with appropriate geometric design of the resonator, promises very high and very stable mechanical quality. The co-etched resonator / electrode structure of the DRG efficiently maximizes use of the area of the sensor to increase sensing capacitance, and thus also increase the signal to noise ratio; also, the axially symmetric design and nodal support ensure minimal coupling to package stresses.

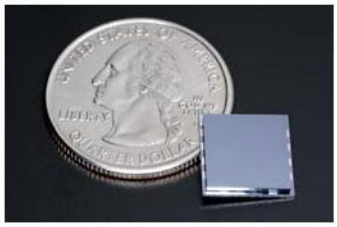

Figure 1.Single axis Disc Resonator Gyroscope (DRG),

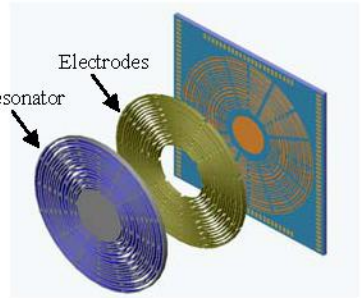

Figure 2 Exploded view of DRG.

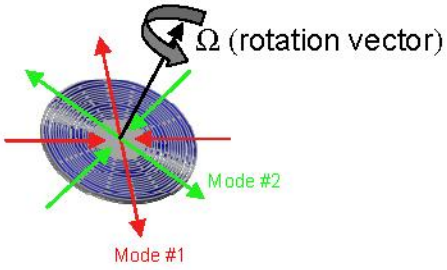

Figure3. Degenerate oscillation modes of resonator ring structure (colored arrows indicate instantaneous direction of motion of mass elements of the ring structure).

The mode #1 of oscillation of the two dimensional ring structures is driven into an oscillating mode along axis (labeled as mode#1 in Figure 1) by sinusoidal actuation via electrodes beneath the plate. In a rotating reference frame the mode#2 of oscillation is coupled to the Coriolis force, which exerts a tangential "force" on the ring. Another set of electrodes beneath the device senses this component of motion along axis (labeled as mode#2 in the figure) 45 degrees to the driven motion. The voltage that is required to

null out this motion is directly proportional to the rate of rotation to which the device is subjected and the voltage scale is reduced proportionally to the frequency split between the two modes of resonance. A change in capacitance occurs as the ring vibrates due to the oscillating gap variation between this ring and the electrodes underneath. This change in capacitance generates a time-varying sinusoidal charge that can be converted to a voltage using the relationship V=Q/C. The ring can be driven around the drive axis by applying a time-varying voltage signal to drive petal electrodes labeled D1-, D1+, D1in-, and D1in+. Because there is symmetry in the device, either of the two axes can be designated as the drive axis. Each mode has a capacitive petal for sensing oscillations as well; driving axis: labeled S1+ and S1-, sensing axis: labeled S2+ and S2-. The micro-gyro has additional plates that allow for electrostatic softening of the silicon springs, labeled B1, BT1, B2, and BT2. Static bias voltages can be used to modify the amount of softening for each oscillation mode. In an ideal, symmetric device, the resonant frequencies of both modes are equal; however, unavoidable manufacturing imperfections in the machining of the device can cause asymmetries in the silicon structure of the device, resulting in a frequency split between the resonant frequencies of these two modes. The frequency split reduces the voltage scale used to measure the rate of rotation to which the device is subjected, and thus the sensitivity for detection of rotation is decreased. By adjusting the static bias voltages on the capacitor plates, frequencies of resonance for both modes are modified to match each other; this is referred to as the tuning of the device using an electrostatic biasing approach [11].

3. DIGITAL CONTROL OF MEMS MICRO GYRO

Gyro Digital Control

As mentioned above, Coriolis forces act on the oscillating ring causing the plane of oscillation to rotate about the Z-axis. The control system measures this rotation by sensing motion around the sense axis (mode#2). Since the amount of rotation is related to the energy sensed in the "sense" direction, the force required to dampen out that motion is again related to the rotation. This process is called sense rebalancing and the amount of energy dissipated to rebalance is quantified as an amount of angular rotation. If the relationship between the sense and drive axes is non-linear, the resultant energy expelled to rebalance the oscillations will also yield a non-linear quantification of the angular rate. As noted previously, modifying the static bias voltages to cause change the spring constant for both modes allows for a closer linear relationship to exist between the vibration modes.

The diagram of the closed-loop control system can be seen in Figure 2. This circuitry includes a drive loop and a sense rebalance loop. The drive loop takes the input from the "drive sense" petal (sensory petal along the drive axis), and outputs the forcing signal to the "drive" petal electrodes (driving force petal along the drive axis). The sense rebalance loop receives input from the "sense" petal (sensory petal along the sense axis), and forces, or rebalances, the oscillations back along the drive axis with a forcing signal to the "sense drive" petal electrode. The magnitude of this forcing function in the rebalance loop is related to the angular rate of rotation. In the figure there are several scaling coefficients indicated K_i, where i ranges from 1 to 8. These constants allow for a mixing of the sensed signals from both axes as described in [1]. We augment the use of these constants by using them to swap the meaning of the drive- and sense-axis, so that the bulk of the energy switches between the two, thus allowing the tuning algorithm to measure the resonance frequency along the X- or Y-axis, or indeed any axis between X and Y. A more detailed description of the operation of this control system can be found in [1].

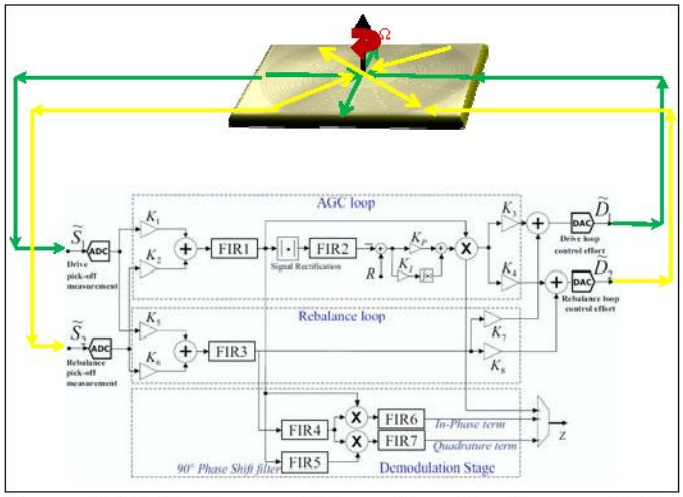

Figure 4. Block diagram of the entire closed-loop control system.

Because the amplitude of the freely oscillating drive axis will naturally decay, another control task is implemented to lightly drive or damp, depending on circumstance, the drive axis so that the amplitude of the driven signal is constant and the gyroscope is maintained in an oscillation mode at the natural frequency. This feature is implemented through an Automatic Gain Control (AGC) loop, shown in Figure 4, combined with finite impulse response (FIR) filters. A signal rectification stage and proportional integrator loop are the main components of the AGC. The output of the AGC is a DC value that modulates the forcing function. The optimal parameters of the FIR filters and the AGC loop to maintain the oscillation of the gyroscope can been determined theoretically using a DSP measurement system and a Matlab modeling tool [12]. The theoretical approach to design filter FIR1 and FIR3 measures the frequency response of all the components and calculates the right

phase. Unfortunately the digital signal processing system combined with the analog circuit create non-linear phase system. Moreover the gyro phase response has a very steep slope of 200deg/ Hz around the resonant frequency, which complicate the filter design.

Gyro Digital Subsystems

The design of the control of the DRG is realized on an FPGA with augmented portability for future designs and implementations.

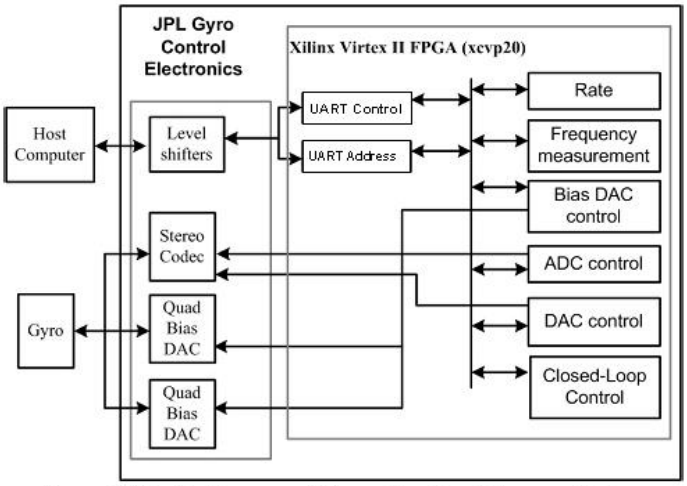

Figure 5. Block diagram of the entire closed-loop control system.

The system used to implement the control, operation, and monitoring of the micro-gyro is referred to as the Gyro Digital System (GDS). Figure 5 illustrates the implementation of the analog and digital systems used to control the micro-gyro. The key circuit elements that allow proper operation of the micro-gyro include the audio codec (Stereo Digital to Analog Converter DAC), high voltage Analog to Digital Converters (ADCs), Universal Asynchronous Receiver/Transmitter (UART) serial interface, frequency measurement and the Digital Signal Processor (DSP) functionality integrated into a Xilinx Virtex II FPGA.

The audio codec is used to translate the analog sensing signals for both the drive and the sense axes. Its stereo capabilities allow for two inputs and two outputs. The high-voltage DACs are utilized for setting the electrostatic bias voltages on the gyro-scope, which range from +15V to -60V. The serial port interface allows for user input/output capabilities. The user can configure the coefficients for the finite impulse response (FIR) filters along with the scaling coefficients (K1 through K8) and automatic gain control (AGC) proportional integral (PI) coefficients (Kp and Ki). The codec is configured through this interface as well.

4. Digital Testing Platform

Our FPGA based digital electronics test platform to implement a real time digital control system for a disc-resonator gyro (DRG) combines a complete software suite and hardware platform

Hardware Subsystems

The Digital Testing Platform includes a FPGA board and FPGA daughter boards. The FPGA board implements the gyro digital control as well as low voltage differential signaling (LVDS) communication between the FPGA and the Gyro boards for high speed over 5 feet long cables. Gyro Board#2 implements the digital to analog and analog to digital converter for the drive and sense signal and using DAC for the Vbias voltages. Gyro Board#1 implements the front-end analog electronics for the gyro. It includes Voltage and Trans-conductance amplifiers.

Figure 6 illustrate the physical and electrical characteristics of the connection between computer and power supplies and FPGA based digital electronics subsystem.

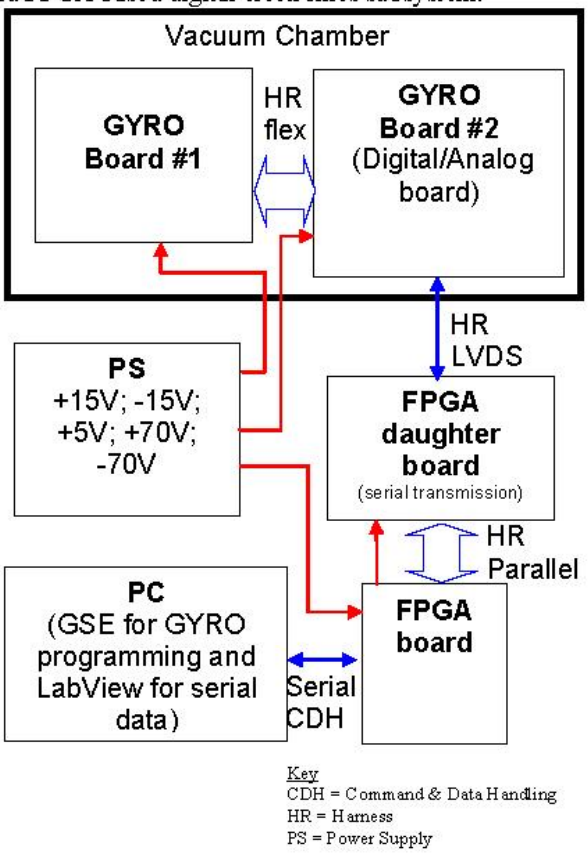

Figure 6. Block diagram of the FPGA DRG Computer PS Physical interface

The power supplies (PS) and computer (PC) provide two electrical interfaces to FPGA digital electronics: the power interface and the command & data handling (CDH)

interface, as shown in Figure 6 and Figure 7. The harness also includes a short connection between the FPGA board and the FPGA daughter. The LVDS communication system allows long lengths (30 feet), between the FPGA electronics boards and the DRG and Pre-Amp board (Gyro Board#1 and Gyro Board#2).

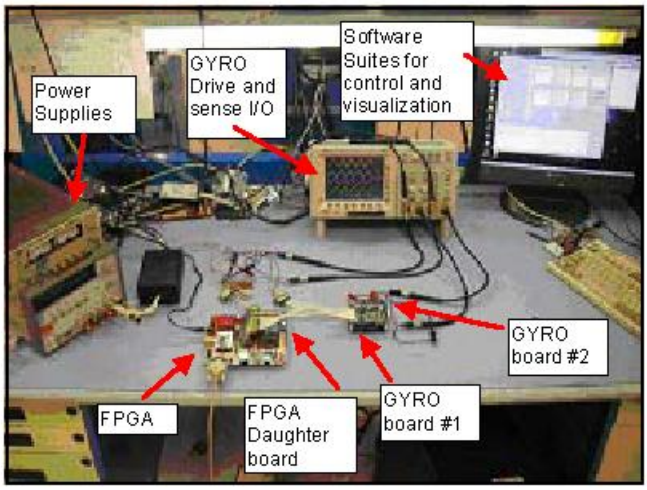

Figure 7. Bench Implementation of the FPGA DRG Computer PS Physical interface

Figure 8 shows the compact implementation of the FPGA and Gyro boards used for the rate measurements on a rate table. For that implementation only the Serial communication with the computer and the power supplies had to be connected to rate table.

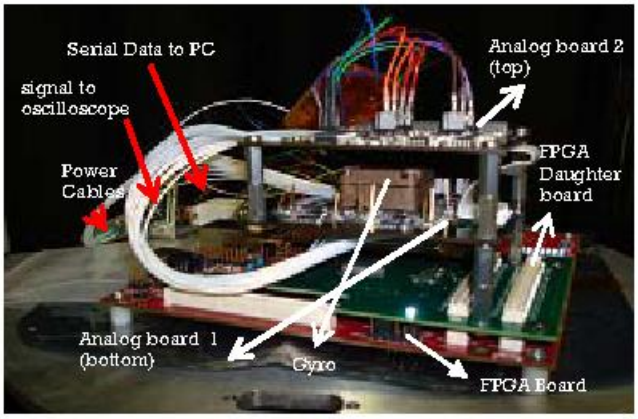

Figure 8. Compact package of FPGA and Gyro boards for evaluation of rate measurement using rate table

Gyro Digital Software Suites

The gyro software, which includes the computer with the host communications software, is connected to the Xilinx FPGA board (hereinafter referred to as the FPGA) via a serial interface. It is made of two software packages: *Gyro Control Interface* and *Gyro Data Logger*. The Gyro Control Interface controls the gyro and reads key signals along the drive and sense signals. The FPGA is in a manual mode where the FPGA can be configured/setup and reports specific data when polled. This is the FPGA's default state on reset/power-up. The Gyro Data Logger is a visualization package to acquire, visualize and log in real-time specific data from the DSP control loop such as the rate and the frequency of resonance. When using the Gyro Data Logger, the FPGA is in an automatic mode: the FPGA will transmit telemetry (i.e. rate, quad, and frequency data) continuously without the need for commands from the software.

When the Gyro Control Interface software starts, the main window on Figure 9 appears. By clicking on COM Check, the operator can ensure that serial communications are working and notice Bytes Sent and Bytes Received in the lower right hand corner: these are good indicators of what level of communication has been achieved. The next step is to choose Write hardware. This simply programs the FIR filters, K coefficients, and codec settings all at once. Note that the bias voltages are NOT programmed with this button. Bias voltages are changed by moving the sliders under Bias Control. Current bias settings may be saved to file, or previously saved ones may be retrieved using the button Load bias... and Save bias.... The last file read from will load by default when the gyro GUI is run.

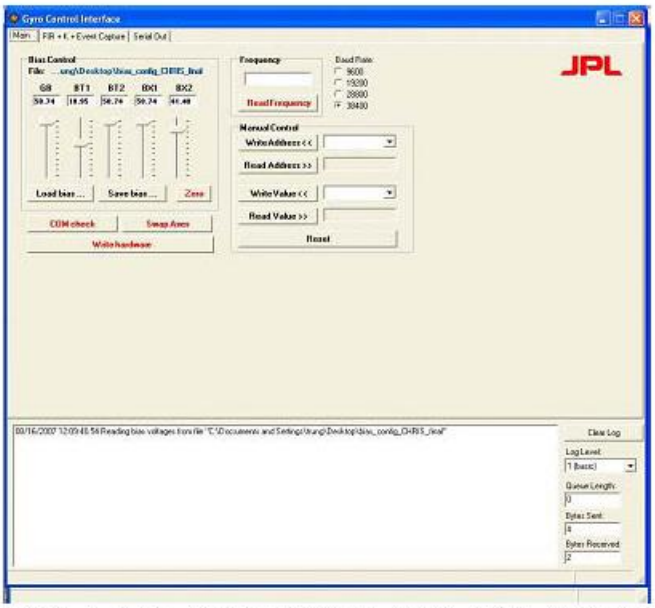

Figure 9. Gyro Control Interface (Main Tab): check the communication, initialize the FPGA registers and program the Vbias.

Next are the FIR + K + Event Capture tab (Figure 10). Here, the operator can change FIR coefficients, K coefficients, miscellaneous registers, and access the Event Capture feature. Note that as long as Dynamic Update is checked (it is by default), moving the sliders will automatically update the FPGA. The operator may move the sliders or type in the textbox to alter values. The text in the textbox will turn red if an invalid value is entered, or if

the value is not verified on the FPGA. Event Capture is available for viewing the internals of AGC operation; it is especially useful in determining whether or not the accumulator is having any effect. As with the bias voltages, the settings on this tab may be saved or loaded, with the last loaded settings being loaded by default when the program is run.

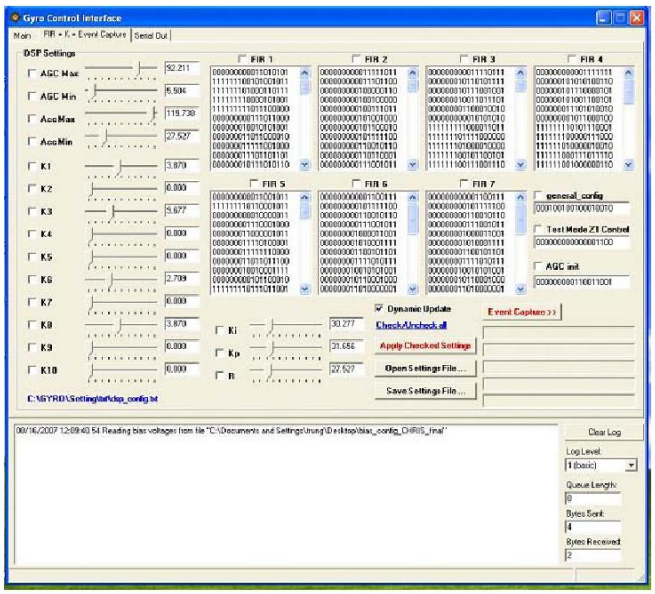

Figure 10. Gyro Control Interface (FIR+K+Event Capture). program FIR filter coefficients, Gain, and capture output of AGC, FIR6 and FIR7.

Once the filter and the gain of the control loop and counter balance loop have been programmed, the operator can switch the FPGA into automatic mode to visualize the rate, frequency and output of filters using the Gyro Data Logger (Figure 11). The telemetry data streamed by the FPGA is organized into packets with 40 headers per packet, ranging from 0 to 39. Each packet is sent every 2.5 ms (limited by the RS232 serial communication between FPGA and the computer in the current hardware configuration)

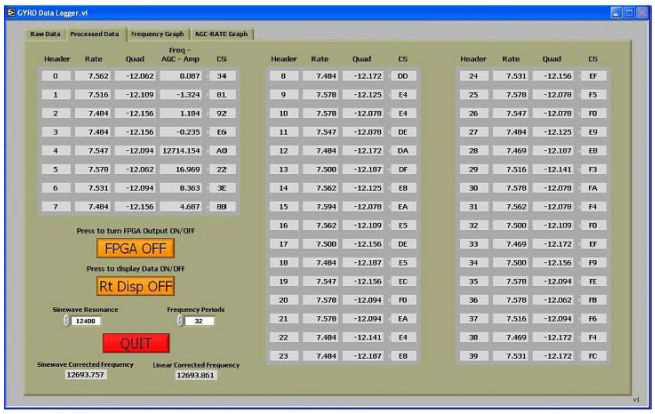

Figure 11. GYRO Data Logger (Processed Data): log of Rate, Quad, AGC amplitude and Resonance Frequency (precision of MHz) of the DRG in real-time.

Figure 12 shows the visualization of the data log. It includes the rate, the AGC, the amplitude of the signal at output of the drive and sense data processing chain.

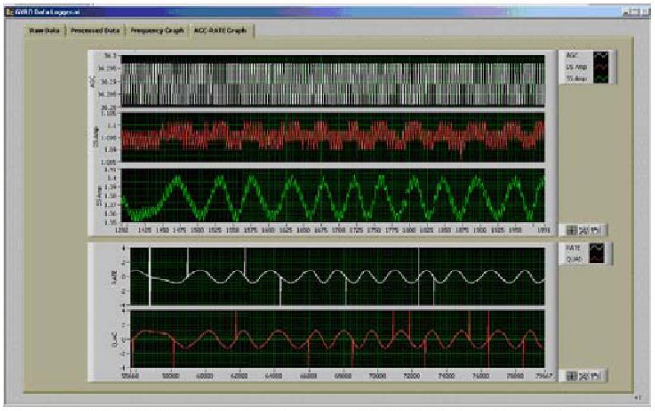

Figure 12. GYRO Data Logger (AGC-Rate Graph): log of Rate, Quad, AGC amplitude and Resonance Frequency (precision of MHz) of the DRG in real-time.

5. Results of Digital Control

Using this FPGA digital control system, the micro-gyro was operated for a period of several hours on a rate table and provided a measurement of the rate as shown on Figure 13. Each lines at the bottom of Figure 13 shows the output in counts of the FIR6 filter for a rotation speed of 0, 1,2,3, … up to 9 deg/s. Each line from the top of Figure 13 shows the output in counts of the FIR6 filter for a rotation speed of 10,20,30,40 and 50 deg/s). The amplitude of the rate measurement (Y-axis) depends on gains (Ks) of the control loop and can be changed to increase the dynamic range of the rate measurement.

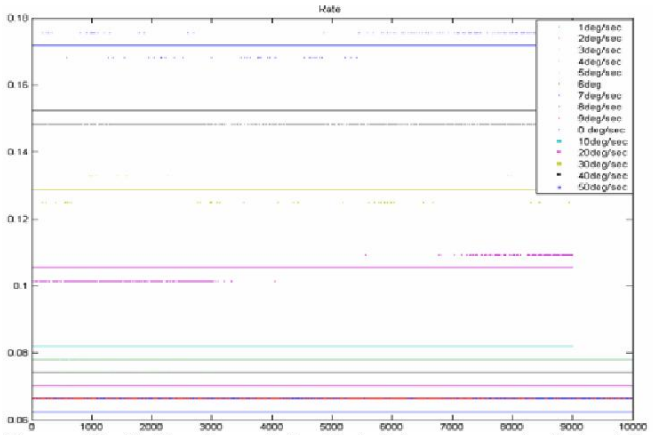

Figure 13. Calibration of the Rate Measurement: Output in counts of the FIR6 filter (Rate) in function of the rotation speed of the rate table.

Figure 14 shows the rate measurement when we changed the rate table speed of rotation by 1 deg/s steps up to 9 deg/s and then by 10 deg/s step up to 90 deg/s. The X axis is the sample number and the Y axis is the raw bin to decimal

values obtained from the rate bit string provided by Gyro Data Logger.

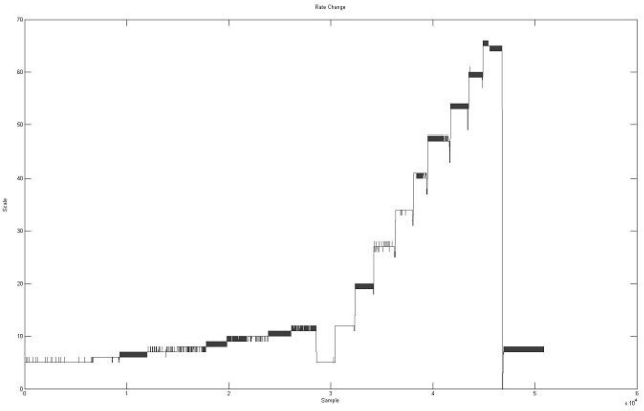

Figure 14. Dynamic RATE measurement: Rate measurements by the FPGA when the speed of rotation of the rate table is changed by 1 deg/s at each of step up to 9 deg/s and then by 10 deg/s steps up to 90 deg/s.

6. SUMMARY

The digital control for MEMS micro-gyroscopes based on FPGAs shows great promise as a technology to replace the cumbersome, less flexible analog control implementation or large high precision data acquisition systems. We demonstrated, using a digital control based on FPGA that we can obtain program and modify in real-time the control loop to adapt to the specificity of each particular gyro and to the change of the mechanical characteristic of the gyro during its life time. Additionally, this architecture could be combined with the "switched drive-angle" tuning method for MEMS gyroscope to allow for in-situ programming and re-tuning of the MEMS micro-gyroscope if there is an unexpected change in the behavior due to radiation, temperature shift, or other faults.

The novel capability of gyro in-situ programming, integrated in a single device next to the gyro, would enable robust, low-mass and low-power high-precision Inertial Measurement Unit (IMU) systems to calibrate during ongoing missions, e.g., Mars Ascent Vehicle.

7. ACKNOWLEDGEMENTS

The work described in this publication was carried out at the Jet Propulsion Laboratory, California Institute of Technology, under a contract with the National Aeronautics and Space Administration. Special thanks to Tom Prince, who has supported this research through the Research and Technology Development grant, entitled "Evolutionary Computation Technologies for Space Systems" and to David Smukowski, president and CEO of "Sensors in Motion Inc." who supported this research through a grant entitled "FPGA based Digital electronics for the Disc Resonator Gyroscope".

REFERENCES

[1] Leland, R.P., "Adaptive mode tuning vibrational gyroscopes", IEEE Trans. Control Systems Tech., vol. 11, no. 2, pp242-247, March 2003.

[2] Painer C.C., Shkel A.M., "Active structural error suppression in MEMS vibratory rate inte-grating gyroscopes", IEEE Sensors Journal, vol.3, no.5, pp. 595-606, Oct. 2003.

[3] Y. Chen, R. M'Closkey, T. Tran and B. Blaes. "A control and signal processing integrated circuit for the JPL-Boeing micro machined gyroscopes" (submitted to IEEE)

[4] R. J. Terrile, et al., "Evolutionary Computation Technologies for Space Systems", in Proceedings of the IEEE Aerospace Conference, Big Sky, March 2005

[5] J.H. Holland, Adaptation in Natural and Artificial Systems, The University of Michigan Press, Ann Arbor, Michigan, 1975.

[6] D. Yuret, M. de la Maza, "Dynamic Hill Climbing – Overcoming limitations of optimization techniques", AI Laboratory, MIT, Cambridge, MA 02139, USA

[7] N. Metropolis, A.W. Rosenbluth, M.N. Rosenbluth, A.H. Teller, E. Teller, "Equation of State Calculation by Fast Computing Machines," J. of Chem. Phys., 21, 1087--1091, 1953.

[8] S. Kirkpatrick, C.D. Gelat, M.P. Vecchi,, "Optimization by Simulated Annealing," Science, 220, 671--680, 1983.

[9] K. Hayworth, "Continuous Tuning and Calibration of Vibratory Gyroscopes", In NASA Tech Brief, Oct 2003 (NPO-30449)

[10] M. I. Ferguson, D. Keymeulen, C. Peay, K. Yee, D. Li, "Effect of Temperature on MEMS Vibratory Rate Gyroscope", in Proceedings of the IEEE Aerospace Conference, Big Sky, March 2005.

[11] K. Hayworth, K. Shcheglov, T. Humphreys, A. Challoner, "Electrostatic Spring Softening in Redundant Degree of Freedom resonators", patent US 6,823,734 B1, JPL and Boeing, Nov. 30, 2004.

[12] R. M'Closkey and D. Kim, "Real-time tuning of JPL-Boeing MEMS gyro", personal communication, JPL, March 2005.

[13] Ed. Kay Stanney, "Handbook of Virtual Environment Technology", Lawrence Erlbaum Associates, 2002.

[14] Didier Keymeulen, Wolfgang Fink,Michael I. Ferguson, Chris Peay, Boris Oks, Richard Terrile, and Karl Yee, "Tuning of MEMS devices using Evolutionary Computation and Open-Loop Frequency Response", IEEE Aerospace Conference, Big Sky, March 2005.

BIOGRAPHY

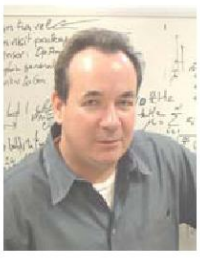

Didier Keymeulen *received the BSEE, MSEE and Ph.D. in Electrical Engineering and Computer Science from the Free University of Brussels, Belgium in 1994. In 1996 he joined the computer science division of the*

Japanese National Electrotechnical Laboratory as senior researcher. Since 1998, he is senior member of the technical staff of JPL in the Bio-Inspired Technologies Group. At JPL, he is responsible for DoD and NASA applications on evolvable hardware for adaptive computing that leads to the development of fault-tolerant electronics and autonomous and adaptive sensor technology. He participated also as test electronics lead, to Tunable Laser Spectrum instrument on Mars Science Laboratory. He served as the chair, co-chair, and program-chair of the NASA/ESA Conference on Adaptive Hardware. Didier is a member of the IEEE.

***Trung Tran** is a University of California at Berkeley student and intern at NASA's Jet Propulsion Laboratory, Pasadena, CA.*

***Phil Withington** is a member of Technical Staff at Jet Propulsion Laboratory, Pasadena, CA.*

***Alireza Bakhshi** is technical expert in FPGA/ASIC and high speed Digital circuit design for real-time DSP application on FPGA. In addition Alireza has twenty years of experience in embedded applications, Digital circuits and Systems design in Space Radiation Hardened, Airport systems and Commercial avionics environments. He has contributed to multiple NASA missions as lead of the digital electronics such as the Microwave Limb Sounder (MLS), Mars Exploration Rover (MER), Ocean Surface Topography Mission (OSTM), Mars Science Laboratory (MSL) flight projects and technology projects such as Ultra Long Life (ULL and, Operation of FPGAs in extreme low temperatures. He is president and CEO of B&A Engineering Inc.*

***Chris Peay** is an Engineer affiliated with NASA's Jet Propulsion Laboratory, Pasadena, CA. His current work is in the areas of control and readout electronics for MEMS vibratory gyroscopes (MVGs) and characterization testing and test automation for MVGs. He received his BS degree in Electrical Engineering from the University of Utah in 1992 and is currently pursuing his MSECE degree at the Georgia Institute of Technology.*

***Richard Terrile** created and leads the Evolutionary Computation Group at NASA's Jet Propulsion Laboratory. His group has developed genetic algorithm based tools to improve on human design of space systems and has demonstrated that computer aided design tools can also be used for automated innovation and design of complex systems. He is an astronomer, the Mars Sample Return Study Scientist, the JIMO Deputy Project Scientist and the co-discoverer of the Beta Pictoris circumstellar disk. Dr. Terrile has B.S. degrees in Physics and Astronomy from the State University of New York at Stony Brook and an M.S. and a Ph.D. in Planetary Science from the California Institute of Technology in 1978.*

***Karl Yee** received his Ph.D. in Theoretical Physics from the University of California, Irvine in 1994. He is a senior researcher within the MEMS Technology group at NASA's Jet Propulsion Laboratory, and has 14 years of experience working on space related projects as an electronic packaging engineer and as a MEMS engineer. He is currently the task manager of JPL's Miniature Gyroscope project.*

***David Foor** is member of technical staff at the Jet Propulsion Laboratory since 2006. He graduated from Texas A&M – Kingsville. As an undergraduate he received a summer research fellowship through the California Institute of Technology where he interned at the Jet Propulsion Laboratory before joining JPL. He is a member of the IEEE Robotics and Automation Society*